The Origin of a Severe Thunderstorm in Kansas on 10 May 1985

FREDERICK SANDERS

Marblehead, Massachusetts

DAVID O. BLANCHARD

NOAA/NSSL/Mesoscale Research Division, Boulder, Colorado

(Manuscript received 2 February 1992, in final form 29 April 1992)

ABSTRACT

This study of the Oklahoma–Kansas area on 10 May 1985 undertakes to explain why severe convection developed in only a small portion of northwestern Kansas despite large potential instability for surface air over the entire region and despite the approach of a mobile upper-level trough from the southwest. Special soundings from the O–K PRE-STORM program showed that a persistent thermodynamic lid above the warm moist surface boundary layer separated this layer from the middle and upper troposphere in which the instability could be realized and was almost completely effective in suppressing deep convection.

Only one of the soundings with these characteristics showed temporary removal of this lid, and the only convective storm developed near the place and time of this removal. This coincidence points to removal as the likely, although not certain, cause. Isentropic trajectories showed that adiabatic lifting was the cause, and that this lift was part of a series of mesoscale waves with wavelengths of about 200 km, vertical extent from 1 to 5 km above the ground, and crests approximately parallel to the wind shear in this layer. The shear was highly ageostrophic, representing a strong transverse circulation in the exit region of a jet streak. Thus, the jet dynamics were responsible only indirectly for the convective outbreak by providing a favorable environmental shear for the directly responsible mesoscale disturbance.

A series of prominent mesoscale oscillations of surface dewpoint along the northwestern boundary of the moist surface layer began coincidentally with the convective development and is considered to have been caused by it.

1. Introduction

On 10 May 1985, indications pointed to the development of severe convection in Oklahoma and Kansas, and the observational facilities of the O–K PRE-STORM (Oklahoma–Kansas Preliminary Regional Experiment for STORM-Central) program (Cunning 1986) were readied. (The project area is seen in Fig. 1.) Only a single group of extremely severe thunderstorms developed in western Kansas, moving rapidly northeastward out of the network, as described by Zacharias (1989). An account by Meitin and Cunning (1985) states ruefully that "this case should prov[id]e valuable data for studying why there was little intense convection within the PRE-STORM network when so many ingredients appeared to be present." This paper reports such a study.

Our approach is to resist the traditional appeal to "indications" or "ingredients" as described in a historical account by Schaefer (1986), however successful it has been in development of the present modest predictive skill. We rely instead on a simple physical consideration: intense convection will occur provided that large convective available potential energy (CAPE) is present in the air column and provided that the typical negative area (CIN, or convective inhibition) below the level of free convection for surface air is somehow removed or reduced to a small value that can be overcome by random cloud-scale pulses at the top of the surface boundary layer. The importance of this inhibiting negative area has been shown by Colby (1980, 1984) and by Carlson et al. (1983). The question is how it was removed in this case. Soundings of the initial structure revealed the "loaded gun" of Fawbush and Miller (1952), characteristic of severe convective situations in the central United States. The relatively dense network of soundings during O–K PRE-STORM appears to have provided an example of a tornado proximity sounding of the type described by Beebe (1958) and a unique opportunity to study how this "smoking gun" came about.

We do not inquire about how the area of large CAPE came about. We do not consider the specific dynamics of the interaction of the cumulus itself with its environment, so the precision with which we can specify the time and place of the outbreak of convection will

Corresponding author address: Dr. Frederick Sanders, 9 Flint St., Marblehead, MA 01945.

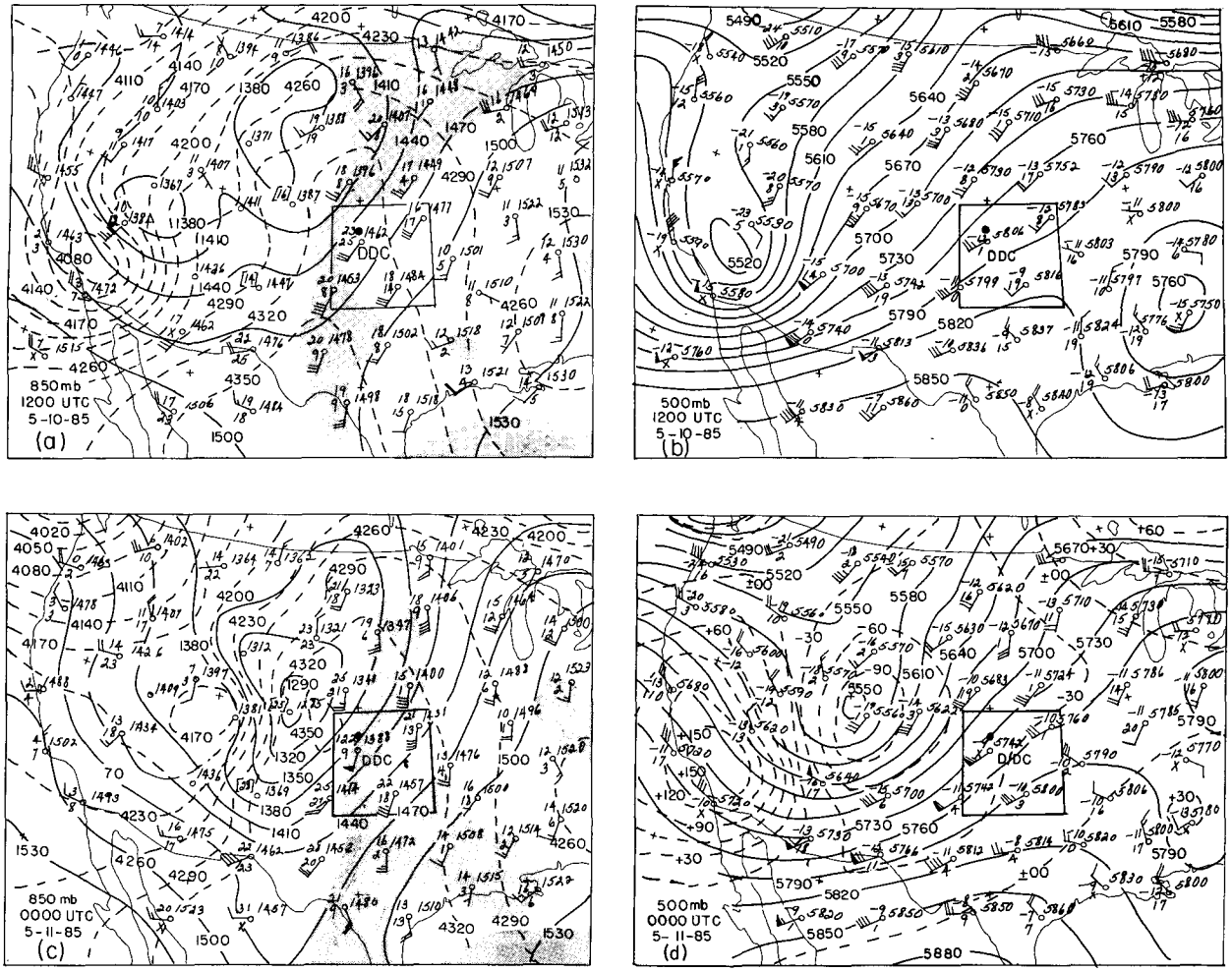

FIG. 1. Analyses at (a) 850 mb and (b) 500 mb at 1200 UTC 10 May 1985. Analyses for the same levels at 0000 UTC 11 May are shown in (c) and (d). The solid lines are height contours and the dashed lines in (a) and (c) are contours of thickness of the layer between these two levels. Dashed lines in (d) are isallohypses for the 12-h period at 30-m intervals. Labels are in meters. The stippled areas in (a) and (c) indicate dewpoints greater than 10°C. The heavy solid line is the boundary of the PRE-STORM observational area. The observation from Dodge City is denoted by DDC and the large dot is the location of the first radar echo at 1936 UTC. The plotting is conventional, with one full wind barb denoting a speed of 5 m s^{-1}. The number at the lower left of the station circle is the dewpoint depression, for which "X" indicates a relative humidity less than the limiting value of 20%.

be limited to an hour or two and to a few tens of kilometers. Finally, we do not ask what kind of convective system develops, although the data are certainly adequate to evaluate the prospects according to the methods advanced by Weisman and Klemp (1982, 1984), Davies-Jones (1984), and Davies-Jones and Burgess (1990). In fact, Davies-Jones and Zacharias (1988) showed that streamwise vorticity in the vicinity of this storm favored its tornadic character.

We focus only on the removal of the negative area and the initiation of intense convection. In so doing, we echo Beebe's (1958) conclusion that "tornado forecasting research . . . must take into account the manner in which the conversion from the precedent sounding to the proximity sounding is effected."

2. The synoptic situation

On the morning of 10 May, there was a broad southerly flow of warm air in the lower troposphere over the central plains, and high moisture in the surface layer extended to 850 mb in or near the western portion of the network (Fig. 1a). During the day, the thickness of the layer from 850 to 500 mb increased in the southerly flow (Fig. 1c), responding to heating of the surface, as a 4350-m center of high thickness appeared near the northwest corner of the area. In the midtroposphere, a sharp mobile trough was in southern California at 1200 UTC. During the following 12 h, this trough moved rapidly northeastward, as seen in Figs. 1b and 1d, with a center of height falls in western Col-

orado and brisk rises on the California coast. This suggests a marginal impact on the northwestern corner of the PRE-STORM area and stronger forced vertical motions to the northwest.

At both 1200 and 0000 UTC, **Q**-vector diagnostics (Hoskins et al. 1978; Barnes 1985) supported this view, indicating weak synoptic-scale ascent (not shown) in Oklahoma and Kansas. The weak forcing is not surprising, considering the small temperature gradient in the broad ridge of warm air shown in Fig. 1. Similar diagnostics by Zacharias (1989) produced comparable results. The thermal wind for the layer from 850 to 500 mb was northerly at about 5 m s^{-1}, corresponding to a horizontal gradient of mean temperature of about 0.3 K (100 km)$^{-1}$. Although the situation was not ideal because the strong synoptic-scale forcing for ascent was too far northwest, the impingement of the forcing on a region of considerable instability made for a difficult forecast decision. Significant convection could not be forecast with assurance, but neither could it be dismissed as unthreatening (or unpromising).

3. A closer look

Routine surface stations and the special mesonetwork delineated a filament of especially moist air in the southerly flow (Figs. 2a–4a), which is bounded to the east by cooler and drier air produced by previous convection (Fig. 2b) and to the west by drier and potentially warmer air. At 1800 UTC (1200 CST), the western contrast in dewpoints was sufficiently strong to denote the structure convincingly as a dryline (Schaefer 1974a) only in southwestern Kansas (Fig. 2a), but during the afternoon, the contrast strengthened from western Texas to southern Nebraska (Fig. 4a), as often happens. No other prominent mesoscale features were evident in the PRE-STORM area, although a cold front appeared in the area shown in the northwest corner of Fig. 4a.

The radar summaries (Figs. 2b–4b) indicate broadly what happened. Aside from the activity already in progress at 1735 UTC, which was mostly weak and in any event not rooted in surface convection, the only new development in the PRE-STORM area centered on the intense echo appearing at 2035 UTC in western Kansas (Fig. 3b). Its growth, according to the detailed analysis by Zacharias (1989), was extremely rapid, from an origin at 1936 UTC to VIP level[1] 5 only 10 min later. The location of origin was about 75 km north-northwest of the sounding site at Dodge City, Kansas (DDC). Zacharias (1989) also notes the initiation of a nearby second cell at 2114 UTC, about 120 km north of DDC, also shown in Fig. 3a. It reached an intensity of VIP level 6 after 30 min, merged with the first storm by 0000 UTC, and never appeared as a separate entity in the radar summaries.

The special PRE-STORM rawinsondes made possible an unprecentedly detailed description of the state of the atmosphere and its evolution in this case. In the analysis of soundings, we addressed only convection originating from surface air. The rationale for using the surface data rather than the mean over some depth of the boundary layer was discussed by Sanders (1986).

For each sounding, the surface parcel was lifted dry adiabatically to condensation, then lifted pseudoadiabatically. The virtual temperature of the lifted parcel was compared with the ambient value up to the level above which it was always colder than its environment. In some instances where the sounding terminated in the upper troposphere at a level where the lifted parcel was warmer than the environmental air, the structure was estimated by interpolation in time. Integrals, with respect to the environmental temperature, of the fractional excess and deficit of parcel temperature were separately evaluated, yielding positively (CAPE) and negatively buoyant (CIN) areas, respectively, on a thermodynamic diagram. Results appear in parts (c) and (d) of Figs. 2–4. Small contributions from the surface boundary layer aside, the positive area (provided it existed at all) extended typically from about 700 to 200 mb, while the negative area (undefined if there was no positive area) lay from about 850 to 700 mb.

Since the integrals represent energy, they can be interpreted as the kinetic energy of vertical motions. The vertical motions have an intuitive appeal absent in energy units and can be obtained by taking the square root of twice the energy value in joules per kilogram. The positive area represents the hypothetical updraft at the top of the positive area starting from rest at the base, with no account taken of dilution, condensate loading, or perturbation-pressure forces. With similar assumptions, the negative area represents the lower limit of the vertical velocity that a parcel would require on entering the base of the layer in order to penetrate it. As illustrated by contours of vertical motion in Figs. 2d–4d, positive areas were found to range upward to near 100 m s^{-1}, whereas negative areas were as large as 30 m s^{-1}. Since the typical boundary-layer parcel velocities of cloud scale at the base of the negative layer are a few meters per second at most, it is clear that only a small negative area is sufficient to inhibit the initiation of convection, as noted by Colby (1980).

In preparing the analyses along the western edge of the positive area in Figs. 2d–4d, close attention was paid to the surface dewpoint analyses so that the effect of the drier air to the west was taken into account as well as possible. The temporal continuity of this positive area was quite clear. The elongated region of explosive convective potential intensified slowly from 1800 to 0000 UTC, reflecting a slow increase in the heat and moisture content of the surface layer. The zone of sharp drop of negative area evidently coincided

[1] VIP levels 1–6 correspond to reflectivities of 20, 30, 41, 46, 50, and 57 dBZ.

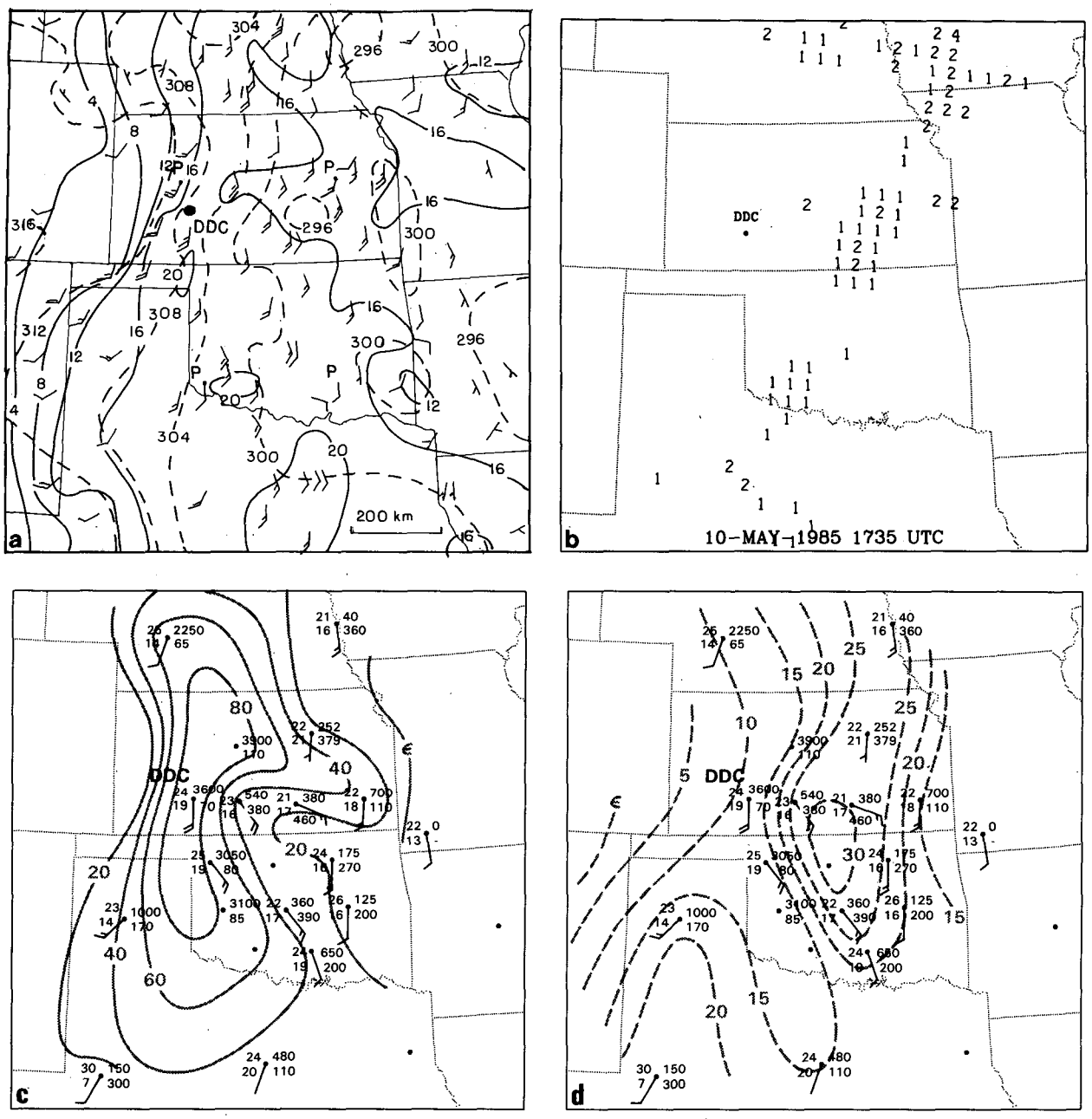

FIG. 2. For 1800 UTC 10 May, (a) analysis of surface potential temperature (dashed lines) at 4-K intervals and dewpoint (solid lines) at 4°C intervals. Surface winds are plotted conventionally for routine stations and for four corner stations of the surface mesonetwork denoted *P*. The location of DDC is indicated, as is the location of the first radar echo at 1936 UTC. (b) VIP levels from manually digitized radar. (c) and (d) Isopleths of negative area (dashed at intervals of 5 m s^{-1}) and positive area (solid at intervals of 20 m s^{-1}) for surface air. The plotted data at each station include the surface wind and the values of the positive and negative areas in joules per kilogram.

with the zone of sharp decrease of positive area, or lay just west of it, since extensive deep convection did not occur. Even this set of special soundings, however, was not sufficient to document the situation with certainty.

There was a single clear exception. Note that the modest negative area (12 m s^{-1}) at DDC at 1800 UTC had vanished by 2100 UTC. The soundings for these two nominal times are shown in Fig. 5. The prominent capping inversion at the earlier time was much weakened and higher at the later time, although it continued to encompass the range of potential temperature around 310 K. The positive area grew from 85 to 93 m s^{-1} during this period because of warming and moistening of the surface boundary layer and despite

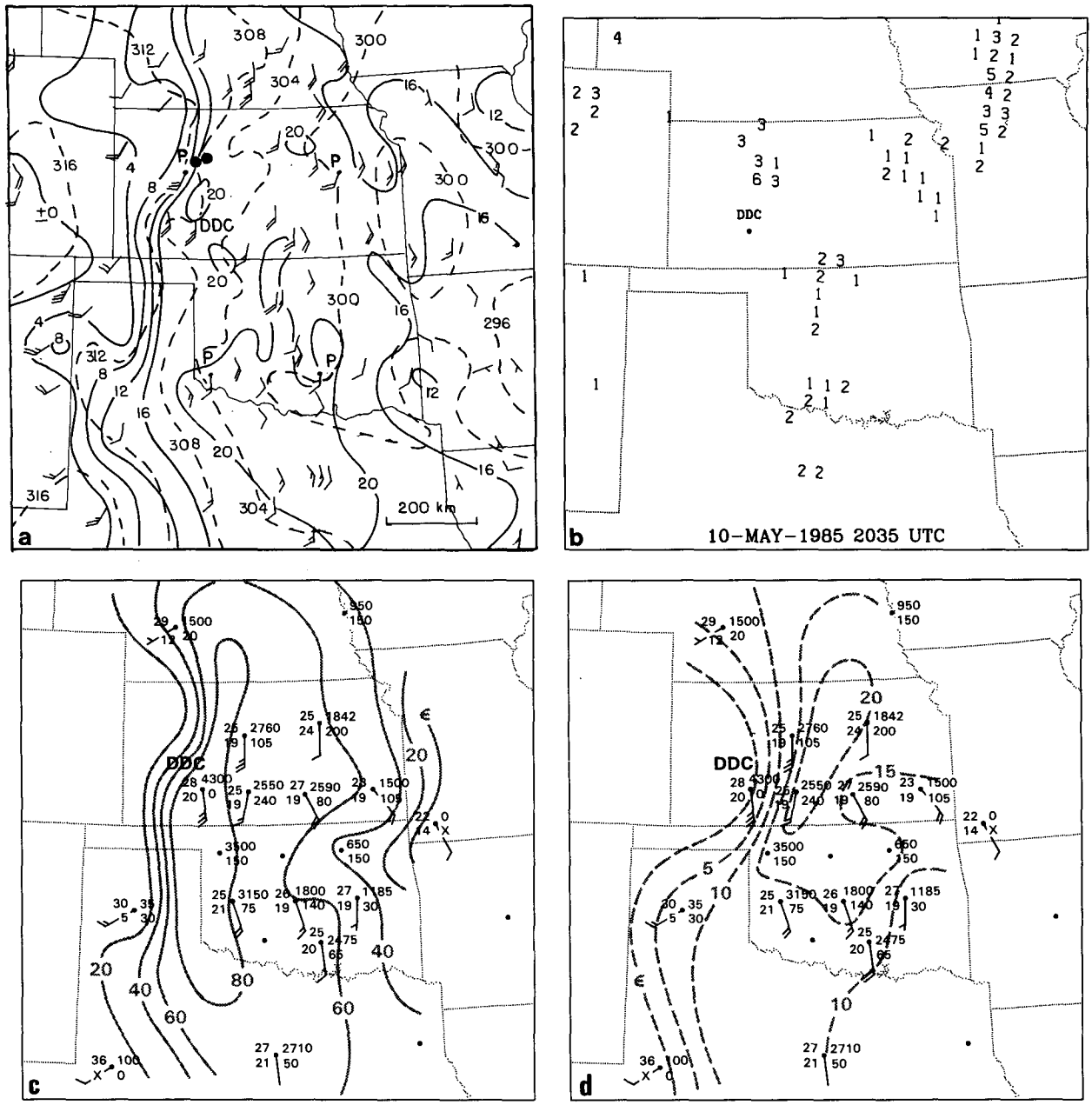

FIG. 3. Same as Fig. 2 but for 2100 UTC 10 May. In (b) the dots represent the locations of the two storm echoes at this time.

slight warming above the lid. Since this station was almost directly upwind in the low-level flow from the sudden severe thunderstorm development noted above, the disappearance of the negative area was almost certainly related to the nearly simultaneous outbreak of intense convection.

A substantial negative area had reappeared at DDC by 0000 UTC (Fig. 4c), and a shallow capping stable layer was lowered to 850–827 mb (not shown). No other sounding with substantial positive area in the PRE-STORM network showed disappearance of the negative area at the times shown in Figs. 2–4 or at 1930 or 2230 UTC when observations were made at a limited number of stations (not including DDC, unfortunately). No other new radar-observed convection occurred in Kansas or Oklahoma.

The answer to the problem posed by Meitin and Cunning (1985), then, is simply that the negative area over almost all the region of large CAPE remained in place. The brief removal shown by the 2030 UTC DDC sounding represents the "smoking gun," and the problem becomes the question of why it was fired. In ad-

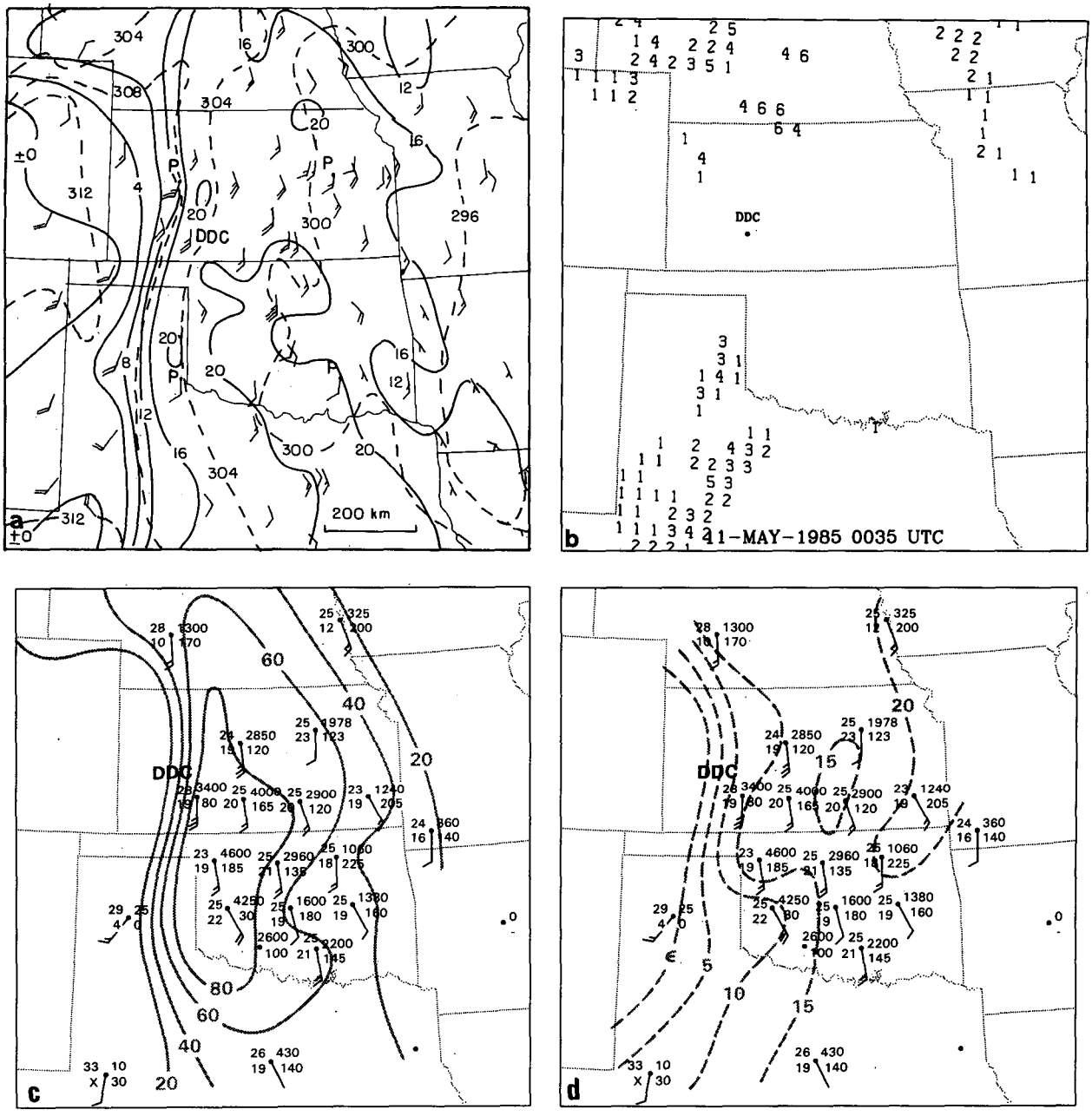

FIG. 4. Same as Fig. 2 but for 0000 UTC 11 May.

dition to Beebe (1958), Bluestein et al. (1988, 1989, 1990) made isolated soundings in the immediate vicinity of intense convection that likewise show no negative area, but the network of PRE-STORM soundings, adjacent in space and time to the crucial one, makes this case a unique opportunity.

4. Mechanisms

A negative area can be eliminated simply by heating the boundary layer until "convection temperature" (Petterssen 1956, p. 140) is reached, with no modification above. That was probably not the case here because surface temperatures in the PRE-STORM area never became sufficiently warm. It can be seen in Fig. 5 that convection temperature for the 1745 UTC sounding was about 31°C, 3°C warmer than the temperature reached at 2030 UTC. We will see, however, that temperatures in the mesonet adjacent to the outbreak approached this value, hence our lack of certainty.

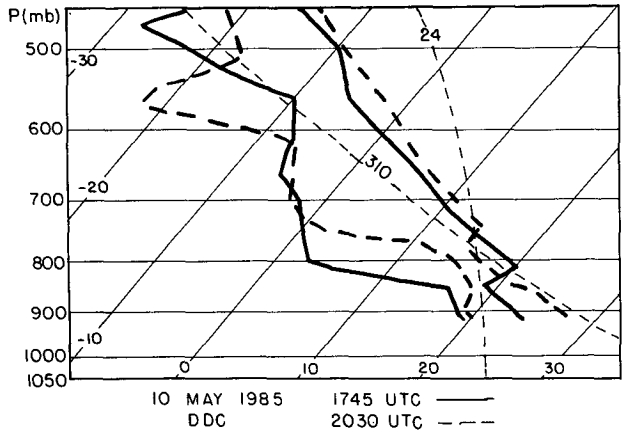

FIG. 5. Soundings of temperature and dewpoint for DDC at 1745 UTC (solid) and 2030 UTC (dashed) plotted on a skew T–log$p$ diagram. A reference dry adiabat, for potential temperature 310 K, and a saturation adiabat, for wet-bulb potential temperature 24°C, are shown as thin dashed lines.

Otherwise, the removal of the lid over the moist surface layer must be a consequence of an ageostrophic circulation. The ascending limb may produce adiabatic cooling of the lid while having little effect on the boundary layer. The horizontal limb may lead to an advance of the boundary-layer air out from under the lid, in the "underrunning" scenario of Carlson et al. (1983). This mechanism requires that at the level of the lid, the air must be colder to the west than in the lid area itself. Since in this case the air to the west was evidently slightly warmer, we are left with adiabatic ascent as the likely mechanism for the cooling shown in Fig. 5 between 830 and 760 mb.

5. Isentropic analysis

Pressure distributions on the 310-K isentropic surface before and after the disappearance of the negative area at DDC are shown in Fig. 6. At 1800 UTC, the pressure increased monotonically from east to west across Kansas to just west of DDC, where the surface descended abruptly to the ground. (No attempt was made to portray possible superadiabatic structure in the drier air to the west.) In Oklahoma, some irregularity was indicated, superposed on a general westward increase of pressure.

Three hours later (Fig. 6b), substantial irregularity of the surface from station to station was evident in Kansas. The sharp pressure fall at DDC was one of a series of rises and falls with a zonal wavelength of no more than 250 km. The spacing of the observations does not permit an unambiguous analysis of the variations. Aliasing is possible but the pattern shown is consistent with all the data at this and adjacent times. Although there was some midlevel cloudiness, air at this level was unsaturated and remained above the surface boundary layer. Thus, potential temperature must have been nearly conserved, and since the horizontal flow pattern was relatively smooth, it is clear that the oscillations represent the effects of vertical displacements.

A reasonable analysis of the local oscillations of pressure on the 310-K isentropic surface from 1200 UTC 10 May to 0300 UTC 11 May is documented in Figs. 7 and 8. The lack of soundings between 1200 and 1800 UTC makes it impossible to say with confidence that mesoscale oscillations were not present then, but the variation of pressure with distance was quite smooth at both of these times. Further, there was no evidence of the oscillations in the soundings at UMN at any time, so they may have been restricted to Kansas and Oklahoma. The analysis suggests a period of 3–4 h, not far from the 4.5-h period estimated by Davies-Jones and Zacharias (1988, hereinafter DJZ). Northward and eastward progression at about 20 m s^{-1} is indicated, with wavelengths of 200–300 km in these directions. A northwest–southeast orientation of the waves and a phase speed of about 14 m s^{-1} are thus implied.

The component of the wind from 225° was calculated for each observation at the standard pressure levels from 850 to 300 mb from 1800 to 0000 UTC at all stations in Kansas and Oklahoma. The results, in Table 1, show speeds through the layer below 400 mb were only slightly faster than the phase speed of the waves, so that propagation was slight.

To obtain as complete as possible a picture of the vertical displacements, trajectories were constructed on each of a set of isentropic surfaces at intervals of 2 K from 306 to 320 K for the 3-h periods from 1800 to 2100 UTC and from 2100 to 0000 UTC. Trajectories were selected that began or ended at the location of an observation to minimize uncertainty due to the pressure analysis. For trajectories beginning at such a point, a straight 1.5-h displacement was laid out downstream, with a direction and length corresponding to the 1800 UTC observation. Then interpolation among the observations for 2100 UTC was used to find a direction and speed that when projected backward the length of a 1.5-h displacement would meet the end of the first segment. For observations terminating at an observation point, this procedure was applied appropriately reversed. The trajectories were not difficult to obtain because the variation of the wind, on the scale of the displacement segments, was not large. Finally, the change was noted between pressures at the observation point and the interpolated point.

As an example of the results, Fig. 6c shows the pressure changes along the trajectories from 1800 and 2100 UTC on the 310-K surface applied at the midpoint of each trajectory. Maximum values of about 60 mb correspond to mean vertical motions of about 6 cm s^{-1}. Values were as large as they were, despite lack of propagation of the waves with respect to the mean wind over much of the domain, because of the substantial growth and weakening of the waves and the variability

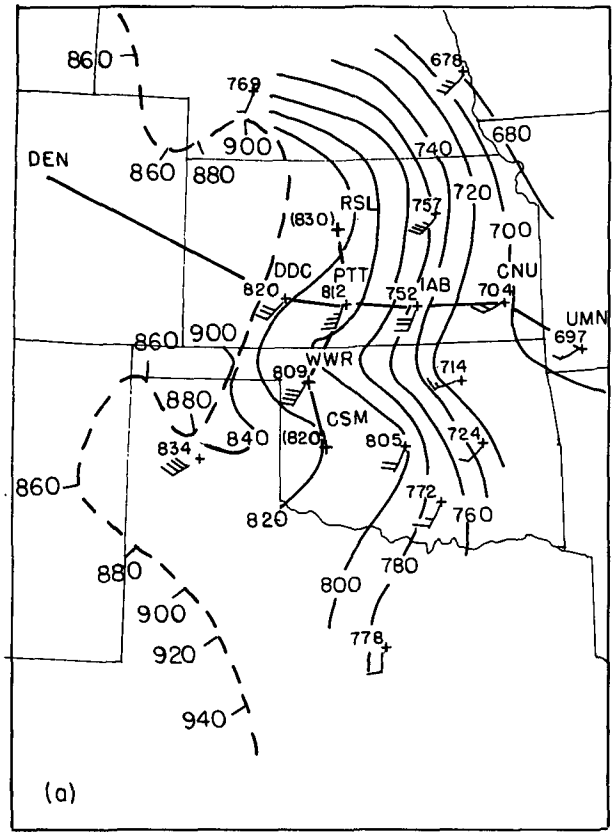

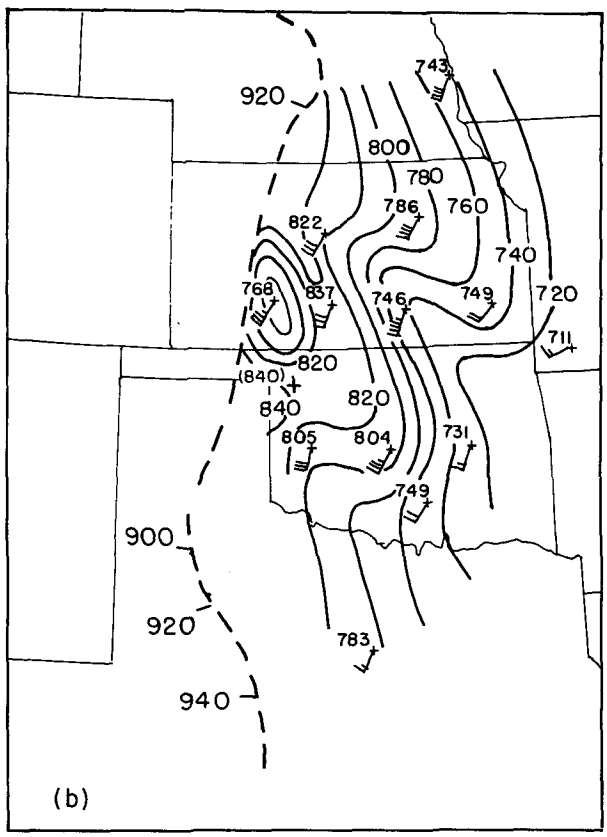

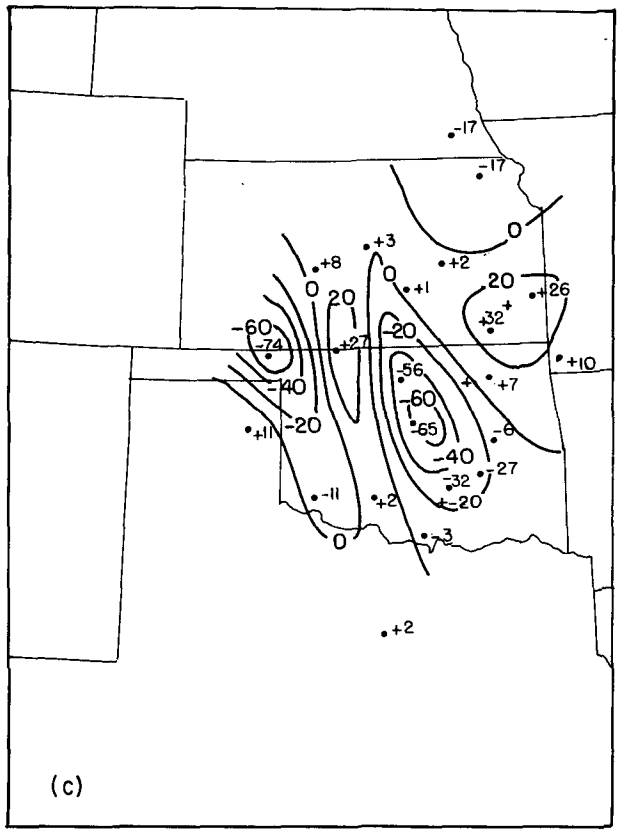

FIG. 6. Isobars on the 310-K isentropic surface for (a) 1800 UTC and (b) 2100 UTC, and (c) 3-h pressure change along isentropic trajectories. Isobars and isallobars are at intervals of 20 mb. In (a) and (b), values at stations are plotted in millibars. Those in parentheses are interpolated from temporally adjacent values. The heavy dashed line is the intersection of this surface with the ground. Pressures at the ground surface are indicated at 20-mb intervals. In (c), displacements are plotted at the midpoints of the trajectories. Location of section lines for Figs. 7 and 8 shown in (a).

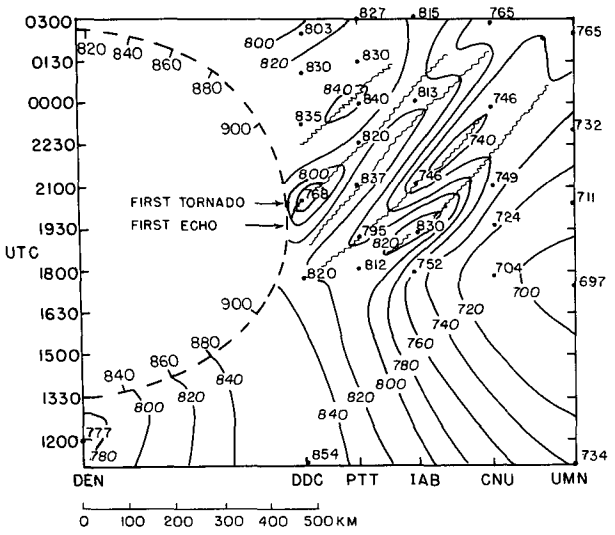

FIG. 7. Time section of the pressure of the 310-K isentropic surface, along the line DEN–UMN indicated in Fig. 6a. Pressure data are plotted in millibars at the time of release of the balloon. Isobars are at intervals of 20 mb. Wavy lines are estimated positions of maxima and minima. The heavy dashed line is the intersection of the isentropic surface and the ground, with pressures indicated at 20-mb intervals.

of the individual wind observations indicated in Table 1. In fact, the mean instantaneous vertical motions were no doubt more intense because of the variability of pressure seen in Figs. 7 and 8 on scales that were not large relative to 3 h.

A vertical cross section of the isentropic surfaces and the vertical displacements is seen in Fig. 9 for the Denver, Colorado, (DEN)–UMN line. The magnitude of the displacements apparently increased above the 310-K surface and then decreased above the 316-K surface.

The results for all trajectories (mostly over Kansas and Oklahoma) and for both periods are illustrated in Fig. 10. For 1800–2100 UTC, the algebraic mean pressure changes were negative, whereas for the period 3 h later they were mainly positive. In both cases, these mean displacements corresponded to vertical motions of no more than 1–2 cm s^{-1}, consistent with the diagnosis of weak synoptic-scale motions discussed earlier. The scatter of individual displacements, representing much larger vertical motions, was a maximum at potential temperature values of 312–314 K in the region from 650 to 600 mb. At all isentropic surfaces, the rms deviations, representing the mesoscale motions, were substantially larger than the mean values.

The apparent maximum intensity of the mesoscale motions in the region from 650 to 600 mb cannot be accepted with full confidence because the small stratification will amplify the effects of errors in the temperature soundings. Above this layer, moreover, the dewpoint depression was often 4°C or less, indicating the possible presence of cloud layers (as also indicated by the satellite imagery and observations from the surface). Therefore, the isentropic trajectories, neglecting the effects of latent heat release or absorption, may have underestimated the magnitude of the vertical motions. In the layer of the negative area, from 306 to 310 K, however, the vertical displacements seem most reliable.

6. The nature of the oscillations

Variations of this sort might be a manifestation of symmetric instability or of ducted gravity-wave activity. Dominance of the latter is not indicated by the very small propagation speed in the domain where the waves were prominent. Although a long gravity wave in the stable layer around the 310-K isentropic level would be evanescent in the well-mixed boundary layer below, this layer was only about 1 km deep. A wave signature would be expected in the data at the ground with higher surface pressure associated with greater elevation (lower pressure) of the isentropic surfaces at a given location. The correlation between changes of surface pressure and of pressure on the 310-K surface was −0.359 from 1800 to 2100 UTC (eight soundings) and −0.559 from 2100 to 0000 UTC (nine soundings). The sign is as expected, but the magnitude is small enough to encourage seeking another explanation. (Even if the phenomenon were determined to be primarily a gravity wave, of course, its source would still need to be identified.)

At first glance, symmetric instability of the type discussed by Emanuel (1979) does not seem promising

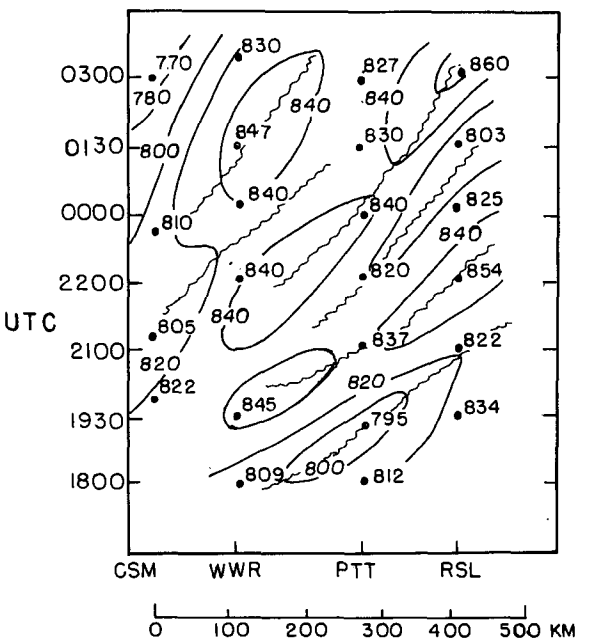

FIG. 8. Same as Fig. 7 but along the line CSM–RSL indicated in Fig. 6a. The isentropic surface did not intersect the ground in this domain.

TABLE 1. Wind components (m s^{-1}) from 225°, Kansas and Oklahoma, 10–11 May 1985. Values in parentheses are rms deviations from mean.

		850 mb	700 mb	500 mb	400 mb	300 mb
Time (UTC)						
1800		14.5 (4.6)	13.6 (6.5)	15.9 (6.7)	18.0 (6.8)	14.3 (9.3)
	N	10	10	10	9	9
1930		14.7 (3.5)	15.3 (5.9)	14.4 (7.8)	19.2 (8.7)	21.4 (8.4)
	N	10	9	9	8	8
2100		14.6 (2.2)	16.0 (6.0)	15.4 (7.3)	19.4 (7.4)	23.0 (9.0)
	N	10	10	10	9	9
2230		14.2 (1.1)	20.3 (5.3)	19.2 (4.6)	23.8 (5.0)	30.3 (8.2)
	N	4	4	4	4	3
0000		18.9 (3.4)	19.0 (6.6)	17.7 (6.7)	21.2 (6.6)	20.6 (7.3)
	N	12	12	12	12	11
All times		15.7 (3.8)	16.5 (6.3)	16.3 (6.8)	20.0 (7.0)	21.9 (8.7)
	N	46	45	45	42	40

in view of the very weak horizontal temperature gradients in the layer from 850 to 500 mb (Figs. 1a,c) and the assumption of thermal-wind balance in the base state. Despite weakness of the thermal wind, soundings of the observed wind in Kansas and Oklahoma began to show a substantial shear in this layer after 1200 UTC, as shown by the analyses in Fig. 11. Initially (Fig. 11a), shears were relatively weak and not grossly out of balance with the thermal wind, although supergeostrophic northwesterly shears could be seen in west-central Texas. These had developed in Kansas and Oklahoma, with magnitudes up to 20 m s^{-1} by 1800 UTC (Fig. 11b), which increase and become more extensive by 0000 UTC (Fig. 11c). All of this occurred with little change in the thermal wind, which remained north-northwesterly near 5 m s^{-1}.

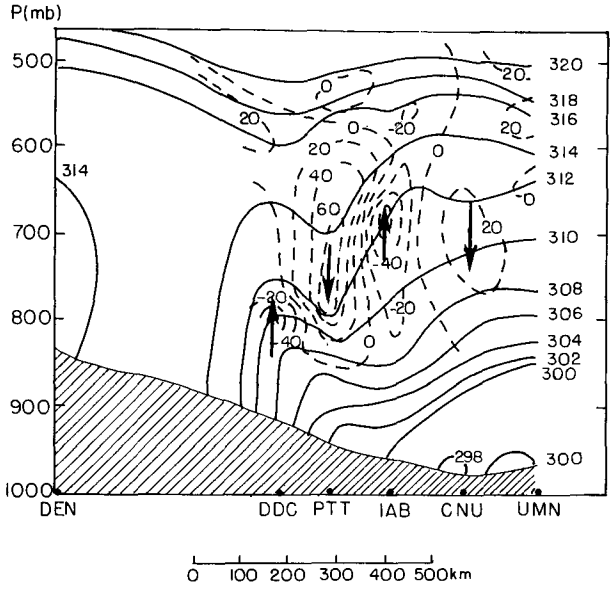

FIG. 9. Vertical cross section of isentropic surfaces (solid) averaged at 1800 and 2100 UTC, and the 3-h isentropic pressure change along trajectories (dashed), for the line DEN–UMN indicated in Fig. 6a.

Examination of the analyses at the two levels in Figs. 1c,d indicates that the ageostrophic shear was attributable to cross-contour flow toward lower height at 850 mb and toward higher height at 500 mb. Qualitatively, it appears that the former was an isallobaric effect in the strengthening southwesterly geostrophic flow ahead of the lee trough, similar to effects noted by Benjamin and Carlson (1986) in numerical simulations. Aloft, the flow in a jet-exit region was reminiscent of that in the case presented by Bluestein and Thomas (1984). The time scale of this ageostrophic shear appears to have been longer than that of the waves on the 310-K isentropic surface, and so might be considered as a base state for them.

The enhanced shear suggests shearing instability as the source of the mesoscale waves. To examine this possibility, Richardson numbers were calculated for each sounding and for each of three nominal isentropic layers, 306–310, 310–314, and 314–318 K, with average depths of about 600, 1900, and 1400 m, respectively. Data from the significant level closest to the isentropic surface were used in the finite-difference approximation,

$$\mathrm{Ri} = \left(\frac{g\delta\theta}{\bar{\theta}}\right)\frac{\delta z}{|\delta \mathbf{V}|^2}, \qquad (1)$$

where $\delta\theta$ is the difference in potential temperature, δz is the difference in height, and $|\delta \mathbf{V}|$ is the magnitude of the vector difference in wind between the two selected significant levels. Calculations were done not only for stations in Oklahoma and Kansas but also for all available nearby observations.

Of the 224 station layers examined, relatively low values of 2 or less occurred 64 times, whereas values lower than 1 were found 16 times. The geographical distribution is illustrated in Fig. 12. West of the PRE-STORM area, the frequency of values of 2 or less exceeded 50%, owing in considerable degree to strong southwesterly shear and small stratification ahead of the jet maximum in the advancing upper trough. In

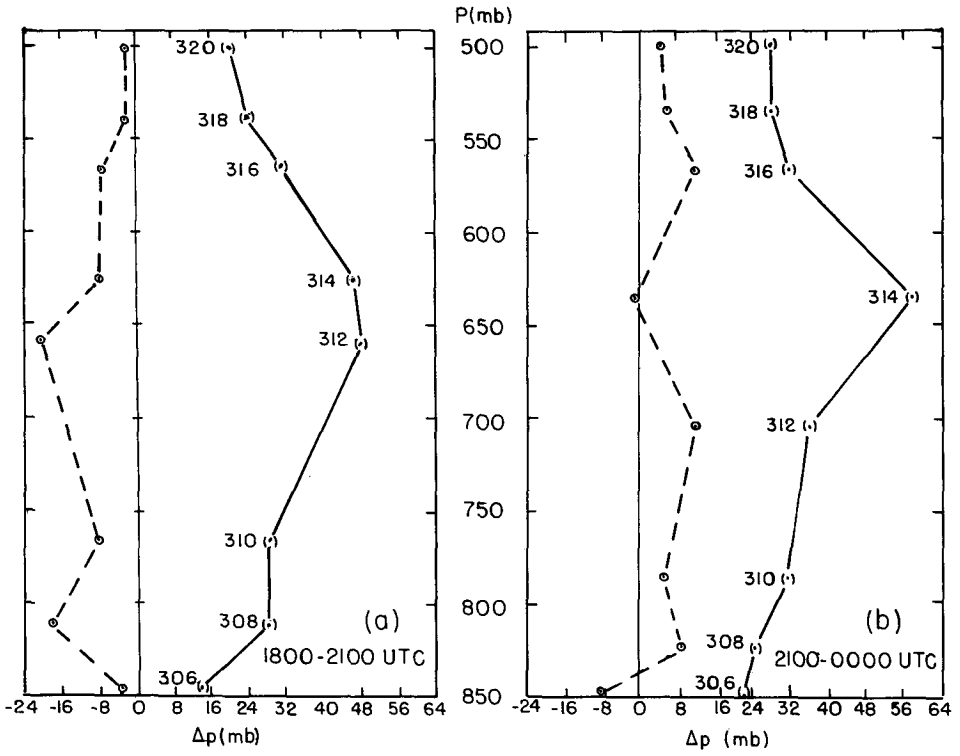

FIG. 10. Pressure changes (mb) along 3-h isentropic trajectories for (a) 1800–2100 UTC and (b) 2100–0000 UTC. Averages over all trajectories for each isentropic surface and period are given by the points connected by dashed lines. Root-mean-square deviations from the average values are given by points connected by solid lines. The plotted numbers are values of potential temperature.

Oklahoma and Kansas, the more modest frequencies were associated with the strong ageostrophic shear shown in Fig. 11. Note that at the peripheral stations north and east of the PRE-STORM area, no very low values occurred. The waves may represent an instability at relatively low Richardson number of the type discussed by Kaylor and Faller (1972).

A further breakdown of the results for Oklahoma and Kansas is presented in Table 2. The greater stratification (smaller depth) of the 306–310-K layer was overbalanced by the strong wind shear to produce somewhat larger frequencies of reduced Richardson numbers here than in the other layers. The stratification of the 314–318-K layer may be overstated because of the presence of cloud in portion of it, as noted earlier; hence, the frequencies may be understated. Except at times when few soundings were available, there was a monotonic temporal increase in the frequencies as the ageostrophic shear developed and strengthened.

Circumstantial evidence thus links the growth of ageostrophic shear on the synoptic scale to the development of mesoscale oscillations of the isentropic surfaces in the negative area overlying the surface boundary layer. These oscillations in turn are linked to the strongly circumscribed outbreak of deep and severe convection.

7. Mesoscale oscillations in the surface data

Zacharias (1989) noted some prominent oscillations in dewpoint recorded by the northernmost stations of the westernmost column in the surface mesonetwork (Meitin and Cunning 1985). He considered them as a possible cause for the convective development but left the question open. In the present study, data from 14 stations were examined in a manner similar to that of DJZ. Locations are given in Fig. 13, showing conditions at the time of first echo appearance. There was weak confluence and a large difference in dewpoint between the northernmost two pairs of stations, consistent with the patterns seen in Fig. 2. The convective system began in this zone of strong contrast, and, despite its phenomenally rapid growth, had little effect on the observations at P1 and P2 at the time of its passage.

It should be noted in Fig. 13, incidentally, that temperatures at P1, P2, and P9 almost reached the convection temperature indicated on the DDC sounding at 1745 UTC, so we must admit the possibility that daytime heating alone was the sole mechanism. The uniqueness of the convective outbreak, however, supports our finding that the lifting of the lid was of crucial importance.

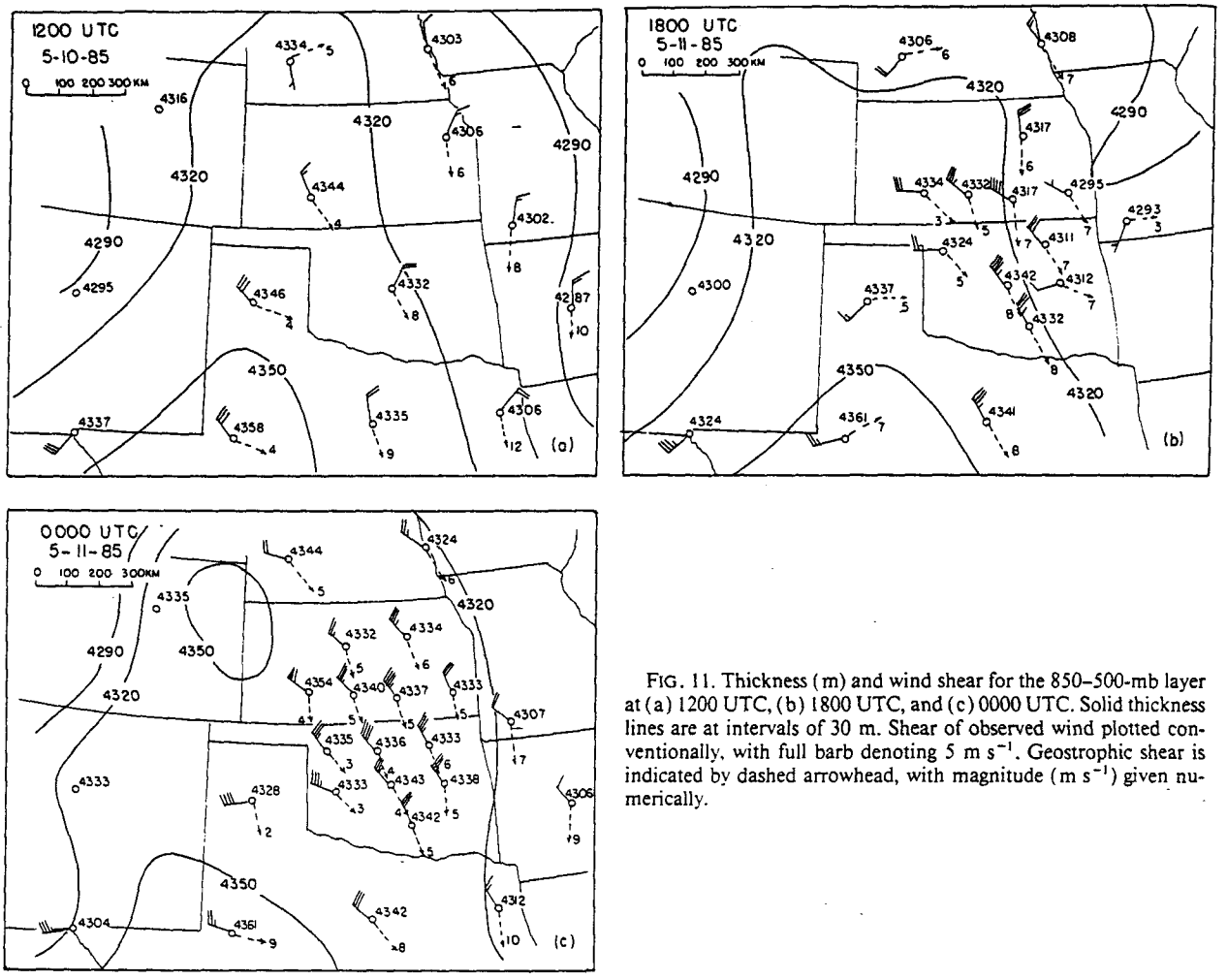

FIG. 11. Thickness (m) and wind shear for the 850–500-mb layer at (a) 1200 UTC, (b) 1800 UTC, and (c) 0000 UTC. Solid thickness lines are at intervals of 30 m. Shear of observed wind plotted conventionally, with full barb denoting 5 m s^{-1}. Geostrophic shear is indicated by dashed arrowhead, with magnitude (m s^{-1}) given numerically.

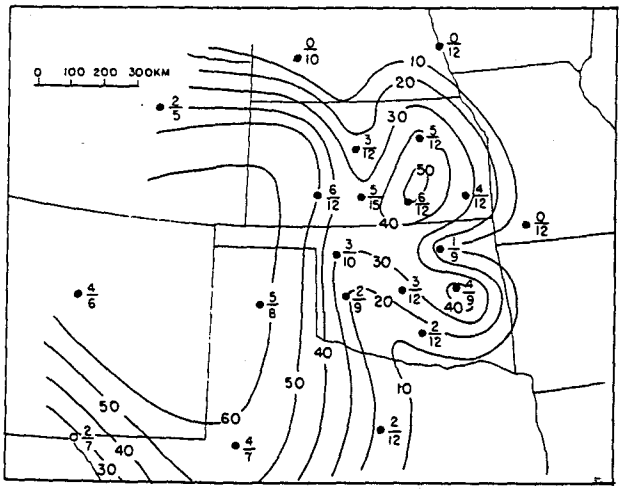

FIG. 12. Relative frequency of isentropic layers with Ri ≤ 2, 1200 UTC 10 May–0000 UTC 11 May. The upper number of the two adjacent to each station location is the number of such values and the lower is the number of layers examined. Isopleths are for relative frequency at intervals of 20%.

Another possibility to be considered is that the lift forced at the dryline by density differences was responsible for the outbreak and also for the oscillations in the lid, as in the case described by Parsons et al. (1991). There, a narrow updraft of about 5 m s^{-1} was estimated at an elevation of 1.5 km over a zone 3 km wide. Such a scenario, as in their Fig. 11, would require a difference of about 10 m s^{-1} in the components of wind normal to the line between stations 3 km apart. It is clear from Fig. 13 that no such difference is observed in the surface winds, even between stations about 40 km apart. Hence, it seems unlikely that this mechanism was operating in this case. Its suppression, even in the presence of substantial density contrasts across the dryline, might be attributable to failure of the strong synoptic-scale forcing to cooperate in this case.

The time series of the dewpoint at the northernmost five pairs of stations, representing the data at 5-min intervals, appears in Fig. 14. Before 2000 UTC, variations aside from secular trends were small and ap-

TABLE 2. Relative frequency of layers with Ri ≤ 2 in Oklahoma and Kansas, stratified by potential temperature and time, 10–11 May 1985. Number of low values and total number of layers are given before and after the solidus, respectively. Values in parentheses are average depths of the layers (m).

Time (UTC)	Potential temperature of layer (K)				
	306–310	310–314	314–318	All	Percentage
1200	1/3 (633)	1/3 (1458)	0/3 (1918)	2/9	22
1800	2/10 (841)	1/10 (1816)	3/10 (1170)	6/30	20
1930	4/10 (681)	2/9 (2097)	2/9 (1219)	8/28	29
2100	4/10 (799)	3/10 (1746)	4/10 (1241)	11/30	37
2230	0/4 (167)	2/4 (2556)	1/4 (1115)	3/12	25
0000	8/12 (464)	2/12 (1745)	5/12 (1617)	15/36	42
All	19/49	11/48	15/48	45/145	31
Percentage	39	23	31	31	

parently erratic at all stations. Dewpoints fell at stations P1 and P9, while rising at all stations in the next column to the east. The result was the strong contrast seen in Figs. 3 and 13.

After this time, a series of relatively large and coherent oscillations began at stations P1, P9, P17, and P25 along the northwest boundary of the network, as noted by DJZ. They represented undulations of the narrow zone of strong dewpoint gradient along the dryline, were most prominent at P1, and did not appear to a significant degree at P33 or to the south or in the next column of stations to the east. (The eastern column of stations displayed a singular northward-moving downward step of dewpoint of 1°–2°C that propagated very little with respect to the low-level flow and did not seem to be related to any convection.) We cannot say there were no oscillations of the dryline to the south because the dewpoint contrast, as seen in Figs. 3 and 4, was west of the surface mesonetwork. The time of onset at P1 and P9, immediately after the appearance of the first echo, supports the idea that the undulations were the result of the convective system rather than its cause.

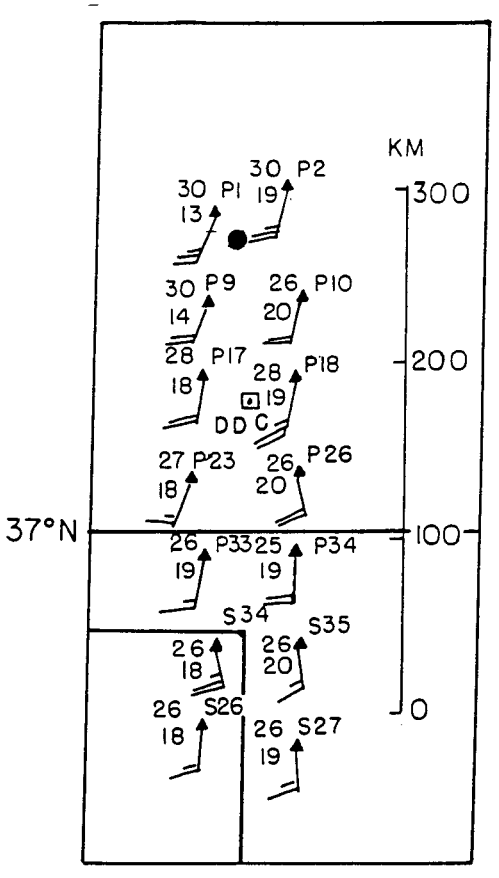

FIG. 13. Conditions in the northwest portion of the mesonetwork at 1930 UTC. Winds, temperatures, and dewpoints are plotted in the conventional manner, and the station designator is plotted above and to the right of the station triangle. The location of DDC is shown, and the solid circle is the location of the first echo appearance at 1936 UTC.

Lag autocorrelation analysis largely confirms the visual impressions. This was separately done for the periods from 1300 to 2000 UTC and from 2000 to 0300 UTC because of the heterogeneous appearance of the time series at P1 southward to P25. Indeed, substantial periodicity, in the range from 140 to 160 min, showed up only at P1, P9, P17, and P25, and there only after 2000 UTC. Lag cross correlations indicated northward movement of the waves at these stations at an average speed of about 20 m s^{-1}, implying a wavelength of about 180 km. Visually, the more prominent troughs showed a slightly smaller period and greater northward speed with a wavelength not much different.

It was not possible to determine the orientation of the wave fronts with confidence. Weak maxima in the east–west cross correlations for the northernmost three pairs of stations, however, suggested eastward propagation at a speed of about 40 m s^{-1}. On this basis, the wave fronts would be oriented west-northwest–east-southeast, with an approximate wavelength of 155 km and speed of 17 m s^{-1}. The flow just above the surface at DDC was from 190° and increasing from 15 m s^{-1} at 2100 UTC to 25 m s^{-1} at 0000 UTC. The propagation of the waves through this flow was therefore probably small. Similar characteristics were found by DJZ.

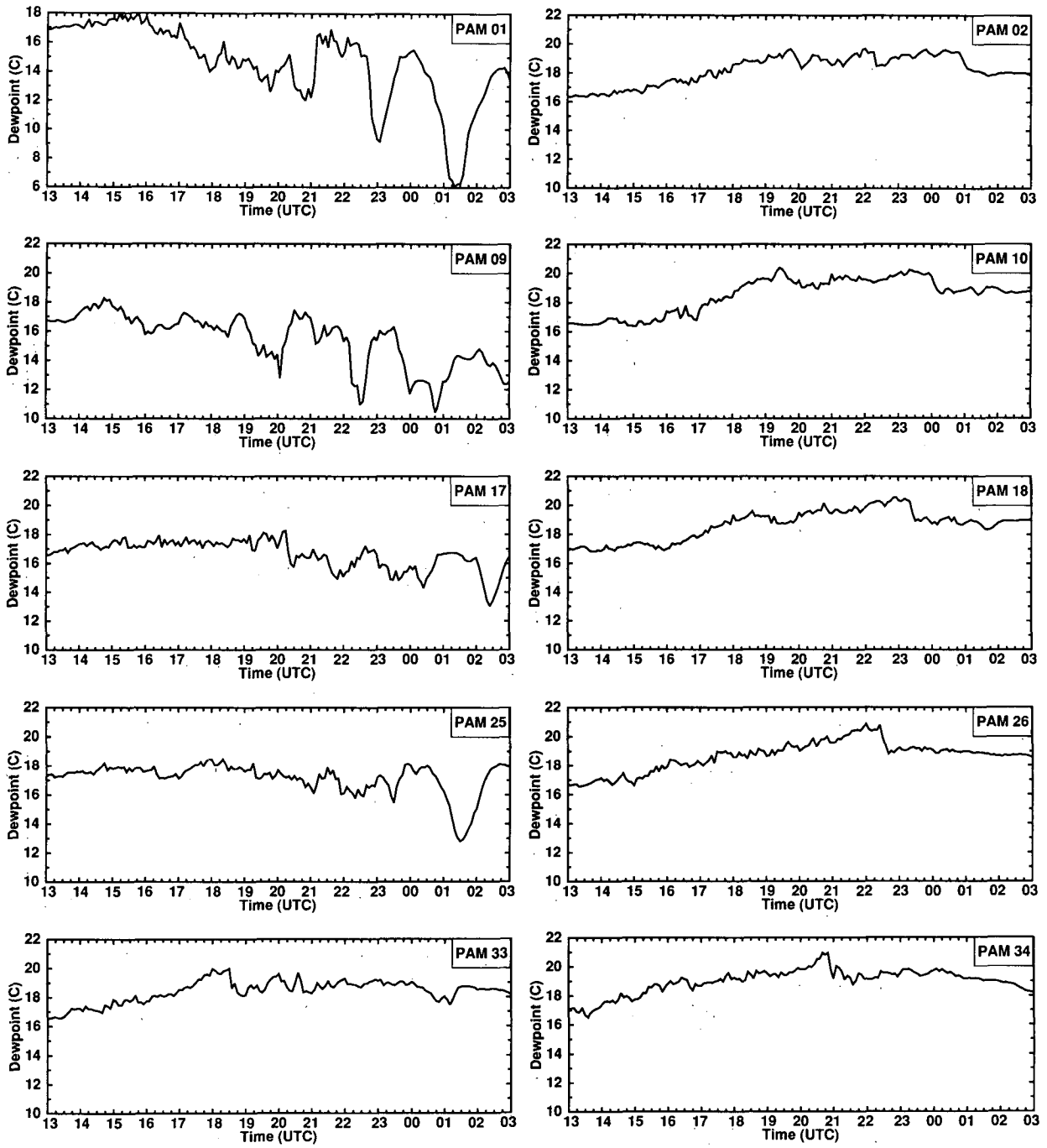

FIG. 14. Time series of dewpoints, 10–11 May, for mesonet stations as indicated. Station PAM 1 is denoted P1 in the text, PAM 2 is P2, etc.

Before 2000 UTC, the correlation analysis suggested a weak 90-min periodicity at P9 and progression toward P1. Indeed, the eye can match some small-amplitude maxima and minima at the two stations (Fig. 14) during the period just before the convective outbreak. The much larger amplitude variations later on, however, failed to produce additional convection in the region, so it does not seem reasonable to assign these waves a causative role.

The zonal components of the surface winds at these 14 stations were examined for two reasons: first, to find whether the waves producing the oscillations in the dewpoint data extended into the region where the moist layer was relatively uniformly distributed and no

prominent oscillations occurred, and second, to see whether the dewpoint oscillations were due to horizontal advection.

The period of oscillation around 140 min was distinct only at P1, P9, and P17 and after 2000 UTC. The waves were moving northward at about the speed noted for dewpoint oscillations. Otherwise, there was considerable high-frequency variability as well as substantial variation on the scale of several hours. Therefore, the disturbances appeared to have been restricted to the zone of strong dewpoint contrast.

If the cause of the dewpoint oscillations were horizontal advection of dry air from the west, then the times series of zonal-wind component and dewpoint should show maximum correlation at a lag of one-quarter period, or about 35 min, with west components accompanying decreasing dewpoints. As the simultaneous plots of dewpoint and component in Fig. 15 show, however, the best match seems to occur near zero lag. Lag correlations for the period 2000–0300 UTC in fact showed maximum negative values at exactly zero lag (although larger negative and positive correlations occurred at P1 with lags corresponding to integral halves of periods). This result indicates that the cause of the oscillations was periodic turbulent transport of drier air and westerly momentum simultaneously to the surface, a process found by Schaefer (1974b) to be primarily responsible for the motion of the dryline. This process was further found by McCarthy and Koch (1982) to play a central role in the development of a severe convective outbreak, but here its role appears to have been reversed. The specific nature of these oscillations is not known, nor can we explain why the circulations that presumably produced them did not initiate further deep convection.

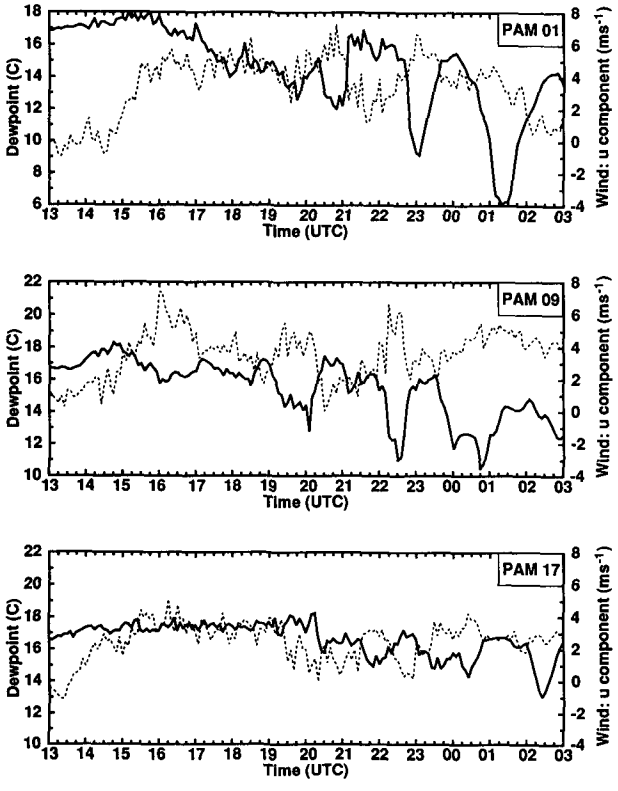

FIG. 15. Time series of zonal component of surface wind (dashed) for mesonet stations P1, P9, and P17, and time series of dewpoint (solid) from Fig. 14.

8. Concluding discussion

We have studied the extremely limited outbreak of severe convection in the O–K PRE-STORM region on 10 May 1985, seeking to understand why the convection developed only in the northwestern corner of the network when large CAPE was present over virtually the entire project area and a strong mobile trough was moving northeastward at upper levels from the southwestern United States. The reason appears to be that a persistent capping thermodynamic lid of relatively warm air separated the warm moist air in the planetary boundary layer from the deep, relatively cool and dry midtroposphere in which the potential buoyancy could be realized.

The qualification reflects the possibility that localized daytime heating alone might have produced the convection, but we do not favor this interpretation. We rely on circumstantial evidence: One of the special PRE-STORM soundings showed that this negative area (on a thermodynamic diagram) was temporarily removed from a limited region in northwestern Kansas. The severe convective storm developed with extreme rapidity within a few tens of kilometers of the location of this sounding and 1 h before the time of the balloon release. Since the sounding from this site 3 h earlier showed only a small negative area, the storm development is viewed as most probably a consequence of its erosion.

Intensive analysis showed that the removal of the negative area was indeed due in part to heating of the surface layer at the sounding site during the daytime, characteristic of the entire region, but also to a very localized lifting of the air comprising the negative area. This lift was a member of a series of mesoscale undulations of the isentropic surfaces in the lid, apparently extending well aloft into the midtroposphere.

The data supported (but did not unambiguously determine) a wavelength of about 200 km and a northwest–southeast orientation parallel to the shear in the layer from 850 to 500 mb above the moist boundary layer with extreme convective potential. The waves propagated very little relative to the flow up to the midtroposphere. The shear was highly ageostrophic, being several times the magnitude of the weak thermal wind over the area. The effect represented the difference between ageostrophic flow across the contours at low levels in response to a locally strengthening horizontal

pressure gradient and cross-contour flow aloft in air traversing the exit region of a jet streak near the base of the mobile upper trough. The strong shear persisted and was responsible for a region of reduced Richardson number in the time and place of the wave activity. The wave development is viewed therefore as a type of shearing instability of a highly nongeostrophic base state.

Research on severe thunderstorms has repeatedly noted the empirical relationship to ascending motion and how the ascent might be diagnosed. This diagnosis often relies on the presence of jet streaks at upper or lower levels or both (Beebe and Bates 1955; Uccellini and Johnson 1979; Bluestein and Thomas 1984; Harnack and Quinlan 1989). Although no detailed physical explanation has been offered in these works for the connection between the initiation of the convective cloud and the larger-scale jet-related ascent, we agree with Doswell's (1987) view that large-scale processes (those that can be understood in terms of quasigeostrophic dynamics) may serve to create the large CAPE but are insufficiently intense to remove the negative area on the observed time scale. Our study indicates that the important effects of the wind structure of jets, however, may not be limited to those produced directly by the associated large-scale transverse circulations. They may produce an environment in which mesoscale disturbances can develop, leading to the convection itself.

Examination of surface data from the special mesonetworks shows prominent oscillations on the part of a dryline close to the convective development, with a period of about 140 min. These grew at the time of onset of convection and are therefore viewed as a *result* of the convection rather than as a *cause* of it. They apparently represented the periodic mixing of dry air and westerly momentum from aloft in the region of strong horizontal moisture contrast but did not lead to further convection. The surface oscillations are not identified with the mesoscale waves aloft, which displayed an apparently longer period but a similar phase speed. The waves in the lid region above the surface layer, moreover, had evidently developed fully immediately before the outbreak of convection and were most intense at some distance from it. These waves, therefore, are regarded as a *cause* rather than as a *result* of the convection.

As far as forecasting implications are concerned, the area of large CAPE could probably be reasonably well inferred from the surface observations and a short-range prediction of the temperature structure at and above 700 mb, as suggested by Sanders (1986). This is not true for the negative area. Continuity of features of the pattern was difficult to maintain aside from the persistent western edge of strong gradient dropping to near zero. It is not clear how the details of its evolution below the region of very large positive area could be inferred from any type of observation other than soundings with detailed vertical resolution. Aside from the difficulties of adequate monitoring, an ability to predict removal of the capping lid would appear to be a necessary prelude to the fulfillment of Lilly's (1990) hope for real-time numerical prediction of thunderstorm systems. The challenge to any kind of forecasting of convection is formidable.

Acknowledgments. The authors are grateful to the PRE-STORM field crew for the outstanding data collection that made this study possible. We thank Barry Schwartz (NOAA/FSL) and Irv Watson (NOAA/NSSL) for providing the software and data for the radar plots and the surface mesonet maps. Discussions of the mesoscale waves with Professor Alan Faller were much appreciated, and we thank Isabelle Kole for skillful drafting of graphics. The research was sponsored in part by the National Science Foundation under Grants ATM-8804110 and ATM-9112727.

REFERENCES

Barnes, S. L., 1985: Omega diagnostics as a supplement to LFM/MOS guidance in weakly forced convective situations. *Mon. Wea. Rev.*, **113**, 2122–2141.

Beebe, R. G., 1958: Tornado proximity soundings. *Bull. Amer. Meteor. Soc.*, **39**, 195–201.

——, and F. C. Bates, 1955: A mechanism for assisting in the release of convective instability. *Mon. Wea. Rev.*, **83**, 195–201.

Benjamin, S. G., and T. N. Carlson, 1986: Some effects of heating and topography on the regional severe storm environment. Part I: Three-dimensional simulations. *Mon. Wea. Rev.*, **114**, 307–329.

Bluestein, H. B., and K. W. Thomas, 1984: Diagnosis of a jet streak in the vicinity of a severe weather outbreak in the Texas Panhandle. *Mon. Wea. Rev.*, **112**, 2499–2520.

——, E. W. McCaul, Jr., G. P. Byrd, and G. R. Woodall, 1988: Mobile sounding observations of a tornadic storm near the dryline: The Canadian, Texas, storm of 7 May 1986. *Mon. Wea. Rev.*, **116**, 1790–1804.

——, ——, ——, ——, ——, G. Martin, S. Keighton, and L. C. Showall, 1989: Mobile sounding observations of a thunderstorm near the dryline: The Gruver, Texas, storm complex of 25 May 1987. *Mon. Wea. Rev.*, **117**, 244–2450.

——, ——, ——, and R. L. Walko, 1990: Thermodynamic measurements under a wall cloud. *Mon. Wea. Rev.*, **118**, 794–799.

Carlson, T. N., S. G. Benjamin, G. S. Forbes, and Y. F. Li, 1983: Elevated mixed layers in the regional severe storm environment: Conceptual model and case studies. *Mon. Wea. Rev.*, **111**, 1453–1473.

Colby, F. P., Jr., 1980: The role of convective instability in an Oklahoma squall line. *J. Atmos. Sci.*, **37**, 2113–2119.

——, 1984: Convective inhibition as a predictor of convection during AVE-SESAME II. *Mon. Wea. Rev.*, **112**, 2239–2252.

Cunning, J. B., 1986: The Oklahoma–Kansas preliminary regional experiment for STORM-Central. *Bull. Amer. Meteor. Soc.*, **67**, 1478–1486.

Davies-Jones, R., 1984: Streamwise vorticity: The origin of updraft rotation in supercell storms. *J. Atmos. Sci.*, **41**, 2991–3006.

——, and D. Zacharias, 1988: Contributing factors in the 10 May 1985 tornado outbreak in northwest Kansas. Preprints, *15th Conf. Severe Local Storms*, Baltimore, Amer. Meteor. Soc., 284–287.

——, and D. Burgess, 1990: Test of helicity as a tornado forecast parameter. Preprints, *16th Conf. Severe Local Storms*, Kannanaskis, Alberta, Amer. Meteor. Soc., 588–592.

Doswell, C. A., III, 1987: The distinction between large-scale and

mesoscale contribution to severe convection: A case study example. *Wea. Forecasting,* **2,** 3–16.

Emanuel, K. A., 1979: Inertial instability and mesoscale convective systems. Part I: Linear theory of instability in rotating viscous fluids. *J. Atmos. Sci.,* **36,** 2425–2449.

Fawbush, W. J., and R. C. Miller, 1952: A mean sounding representative of the tornadic airmass environment. *Bull. Amer. Meteor. Soc.,* **33,** 303–307.

Harnack, R. P., and J. S. Quinlan, 1989: Association of jet streaks and vorticity advection pattern with severe thunderstorms in the northeastern United States. *Nat. Wea. Digest,* **14,** 5–12.

Hoskins, B. J., I. Draghici, and H. C. Davies, 1978: A new look at the omega-equation. *Quart. J. Roy. Meteor. Soc.,* **104,** 31–38.

Kaylor, R., and A. J. Faller, 1972: Instability of the stratified Ekman boundary layer and the generation of internal waves. *J. Atmos. Sci.,* **29,** 497–509.

Lilly, D. K., 1990: Numerical prediction of thunderstorms—Has its time come? *Quart. J. Roy. Meteor. Soc.,* **116,** 779–798.

McCarthy, J., and S. E. Koch, 1982: The evolution of an Oklahoma dryline. Part I: A meso- and subsynoptic-scale analysis. *J. Atmos. Sci.,* **39,** 225–236.

Meitin, J. G., Jr., and J. B. Cunning, 1985: The Oklahoma–Kansas Preliminary Regional Experiment for STORM-Central (O-K PRE-STORM). Volume I. Daily Operations Summary. NOAA Tech. Memo., ERL ESG-20, 313 pp. [Available from Environmental Study Group, Environmental Research Laboratories, Boulder, CO.]

Parsons, D. B., M. A. Shapiro, R. M. Hardesty, R. J. Zamora, and J. M. Intrieri, 1991: The finescale structure of a west Texas dryline. *Mon. Wea. Rev.,* **119,** 1242–1258.

Petterssen, S., 1956: *Weather Analysis and Forecasting. Volume II: Weather and Weather Systems,* 2d ed. McGraw-Hill, 266 pp.

Sanders, F., 1986: Temperatures of air parcels lifted from the surface: Background, application, and nomograms. *Wea. Forecasting,* **1,** 190–205.

Schaefer, J. T., 1974a: The life cycle of the dryline. *J. Appl. Meteor.,* **13,** 444–449.

——, 1974b: A simulative model of dryline motion. *J. Atmos. Sci.,* **31,** 956–964.

——, 1986: Severe thunderstorm forecasting: A historical perspective. *Wea. Forecasting,* **1,** 164–189.

Uccellini, L. W., and D. R. Johnson, 1979: The coupling of upper and lower tropospheric jet streaks and implications for the development of severe convective storms. *Mon. Wea. Rev.,* **107,** 682–703.

Weisman, M. L., and J. B. Klemp, 1982: The dependence of numerically simulated convective storms on vertical wind shear and buoyancy. *Mon. Wea. Rev.,* **110,** 504–520.

——, and ——, 1984: The structure and classification of numerically simulated convective storms in directionally varying wind shears. *Mon. Wea. Rev.,* **112,** 2479–2498.

Zacharias, D. P., 1989: A case study of the 10 May 1985 tornado outbreak in northern Kansas. M.S. thesis, University of Oklahoma Graduate College, Norman, 135 pp.